Journal of Statistical Mechanics: Theory and Experiment
An IOP and SISSA journal

Persistence in practice

J M J van Leeuwen[1], V W A de Villeneuve[2] and H N W Lekkerkerker[2]

[1] Instituut-Lorentz, University of Leiden, PO Box 9506, 2300 RA Leiden, The Netherlands
[2] Van 't Hoff Laboratory for Physical and Colloid Chemistry, University of Utrecht, Padualaan 8, 3584 CH Utrecht, The Netherlands
E-mail: jmjvanl@lorentz.leidenuniv.nl, vdevilleneuve@hotmail.com and h.n.w.lekkerkerker@chem.uu.nl

Received 10 June 2009
Accepted 5 August 2009
Published 9 September 2009

Online at stacks.iop.org/JSTAT/2009/P09003
doi:10.1088/1742-5468/2009/09/P09003

Abstract. We present a scheme for accurately calculating the probabilities of persistence on sequences of n heights above a level h from the measured $n+2$ points of the height–height correlation function of a fluctuating interface. The calculated persistence probabilities compare very well with the measured persistence probabilities of a fluctuating phase-separated colloidal interface for the whole experimental range.

Keywords: persistence (theory), persistence (experiment), stochastic processes (theory)

J. Stat. Mech. (2009) P09003

Contents

1. Introduction

Persistence is related to the question of how long a fluctuating variable stays above a certain level. This is a recurrent theme in statistical physics. It started as the problem of level crossing in probability theory [1]–[3]. If the problem is posed in the context of Gaussian random processes, persistence is completely determined by the correlation function of the stochastic variable. For these processes the essence of the problem is calculating, from the correlation function, the probability that the fluctuation variable stays above a certain level during the time t. This turned out to be a classic unsolved problem in probability theory [2, 4, 5]. Around the turn of the century the investigations reached a peak, with applications in physics ranging from properties of the diffusion equation [6]–[8], survival of spin states [9]–[11], [4, 12], fluctuating steps [13] and interfaces [5, 14], to persistence in order parameters [18] and non-Gaussian processes [19]. A recent review on equilibrium step fluctuations, which poses the problem of persistence in a wide context, is given by Constantin *et al* [15].

The investigations focused on the calculation of the asymptotic behavior. The associated persistence exponent sometimes characterizes a new partition of physical systems into universality classes. For a stationary Gaussian process the persistence probability for a time t decays exponentially with t. For these processes the persistence probability can be written as the ratio of two path integrals. The numerator involves the sum over paths obeying the condition of persistence and the normalizing denominator over paths without the condition. For a Markov process the correlation function is an exponential and both path integrals can be evaluated. But as yet there is no general scheme for an arbitrary correlation function for calculating the persistence exponent.

doi:10.1088/1742-5468/2009/09/P09003

J. Stat. Mech. (2009) P09003

Most theoretical investigations treat the process as a continuous process in time, which it certainly is. However measurements of a stochastic variable are necessarily discrete in time. One would think that, with a sufficiently high experimental sampling rate, the limit of a continuous process would be seen experimentally, such that the sampling rate would become irrelevant. This is not obvious though, in particular for 'non-smooth' processes [4]. A 'smooth' process has a correlation function deviating from its initial value in a quadratic way. The influence of the discreteness of the sampling on the persistence exponent has been investigated by Majumdar *et al* [16] for stationary Gaussian Markov processes and by Ehrhardt *et al* [17] for a number of non-Markovian smooth processes. In general the exponent derived from discrete sampling is lower than the continuous exponent, because double crossings of the level in between two discrete sampling points are missed. These authors consider the calculation of the persistence of a discrete sequence more difficult than that of the underlying continuous process, as the approximation schemes derived for continuous processes are not applicable to discrete series of data. For 'non-smooth' processes another difficulty arises in the calculation of the persistence probability, because rapid fluctuations give a diverging probability on a short time scale, such that the mean persistence time vanishes [5, 20].

Recently we encountered the persistence problem in an experimental study of a fluctuating interface between phase-separated colloid–polymer mixtures [20]. This is an example of a stationary Gaussian random process, since the fluctuations are small in amplitude and their energy is given by a quadratic Hamiltonian in the stochastic variables. On the time scale of the measurements the process is non-Markovian and non-smooth. We have collected data on the correlation function and on the joint probabilities for, e.g., finding n successive height values above the level h. Thus here the practical persistence problem presents itself in a discretized form and the question arises of whether one can calculate, from the values of the correlation function, directly, the persistence probabilities of the same set of points in time. In an earlier publication [21] we demonstrated how to do this for short series. In this paper we extend the calculation to the whole set of experimental points. We focus here on the longer time sequences which allow for more detail than the similar spatial sequences. We find the values of the correlation function at equidistant time intervals and also the persistence probability for the same series of time steps.

Thus experimental data were obtained in large numbers and with high accuracy for an interesting system, which enabled us to further test the theories on the persistence problem. As mentioned in [17], the continuum limit usually leads to a simplification of the calculation, but we find in our case the discreteness of the experimental data rather a blessing in disguise. Our aim is to show how the persistence probabilities for n events can be directly calculated from the measured $n + 2$ points of the correlation function for the range of measured points, which are neither on a short time scale nor in a fully asymptotic regime. We derive two sum rules for the discrete series, which play a vital role in assessing the accuracy of the computational scheme.

2. The experimental system

Traditionally experimental studies of interfaces are carried out by means of light and x-ray scattering. The field obtained another dimension from experiments of Aarts *et al*

J. Stat. Mech. (2009) P09003

[22, 23], in which they obtained microscopic images of fluctuating interfaces of phase-separated colloid–polymer mixtures using confocal microscopy. Although scattering on interfaces is most valuable, it always yields *global* information on the fluctuations, while inspection by microscopy gives *local* information. However, the wavelengths and heights involved in the capillary waves of molecular fluids are way beyond the reach of detection by microscopic methods. For colloidal interfaces the characteristic length and time scales of the fluctuations can become accessible via confocal microscopy, on lowering the surface tension to the nN m^{-1} range.

Here, confocal microscopy measurements were performed on phase-separated colloid–polymer mixtures. The colloids are 69 nm radius fluorescently labeled polymethylmethacrylate particles, suspended in *cis/trans* decalin, with polystyrene (estimated radius of gyration = 42 nm) added as a depletant polymer. Due to a depletion induced attraction, these mixtures phase separate at sufficiently high colloid and polymer volume fractions and an appropriate colloid to polymer aspect ratio into a colloid-rich/polymer-poor phase (colloidal liquid) and a colloid-poor/polymer-rich phase (colloidal gas) [24]. Here the polymer concentration acts as an inverse temperature and upon dilution the binodal is approached.

In confocal microscopy a monochromatic laser beam is used to excite dye molecules attached to (in this case) the colloid. Through a dichroic mirror the outgoing light is separated from the incoming light. A two-dimensional confocal slice is then obtained through a pinhole, from single-wavelength fluorescent light emitted from the sample. For our experimental system, the confocal slices are only three colloidal diameters thick; the density profile between the two phases is observed as a function of fluorescence intensity.

A very precise location of the interface can be obtained by fitting the intensity with a van der Waals profile: $I(z,x) = a + b\tanh([z - h(x)]/c)$, where z is the direction perpendicular to the interface and x a coordinate along the interface. In the upper phase the density approaches a value corresponding to $a + b$ and in the lower phase, one corresponding to $a - b$, while c measures the intrinsic width of the interface. Thus at every snapshot a function $h(x)$ follows and the sequence of snapshots gives the function $h(x,t)$. This is a practical separation of the particle motions, which lead at short scales to the *intrinsic interface* and the particle motions (*capillary waves*) which drive the long wavelengths. This opens up the possibility of following in detail the motion of the height of the interface and of making a statistical analysis of its temporal behavior. Of course the method has its inherent restrictions. Just as in ordinary movie recording, snapshots have to be taken at finite time intervals. For colloidal interfaces this interval can be made much smaller than the intrinsic time scale of the motions.

With a Nikon E400 microscope equipped with a Nikon C1 confocal scanhead, several series of 5000 snapshots of the interface were recorded, at constant intervals Δt of 0.45 s and 0.50 s, for two state points to be denoted as II and IV. The latter is closer to the binodal. The pixels are separated by a distance $\Delta x = 156$ nm and a single scan takes approximately 0.25 s to complete. With 640 heights per snapshot, we obtain in total 640×5000 data points, which enable us to measure persistence probabilities as low as 10^{-6}.

J. Stat. Mech. (2009) P09003

3. The correlation function

We write the normalized correlation function as

$$g(t/t_c) = \langle h(0,t)h(0,0)\rangle / \langle h^2\rangle, \tag{1}$$

where $\langle h^2\rangle$ is the equal time correlation function. t_c is the characteristic time of the process which we have inserted in the argument of g to make it dimensionless. It is given by the expression

$$t_c = \frac{(\eta + \eta')}{\sqrt{g\gamma\Delta\rho}}, \tag{2}$$

where the η s are the viscosities of the two coexisting phases, $\Delta\rho$ the density difference and γ the surface tension. From the definition it follows that $g(0) = 1$. Heights are scaled with $\langle h^2\rangle^{1/2}$ and times with t_c, so we can work exclusively with dimensionless quantities. Experimentally one has a discrete sampling of $g(t/t_c)$ with Δt as the smallest interval. Thus one finds a sequence $g_n = g(n\delta)$ with $\delta = \Delta t/t_c$.

Capillary wave theory for overdamped waves gives the following expression for the correlation function [20, 25]:

$$g(t/t_c) = \frac{2}{\log(1+\kappa^2)} \int_0^\kappa x\,\mathrm{d}x\, \frac{\exp[-(x + x^{-1})(t/2t_c)]}{1 + x^2}. \tag{3}$$

The upper bound of the integral is $\kappa = 2\pi\xi/d$ with $\xi = \gamma/(g\Delta\rho)$ the correlation length and d the diameter of the particles. The lower bound, determined by the size of the system, has been set equal to 0. The upper bound is essential for the convergence of the integral and the influence on the short time behavior of the correlation function. Cutting off the capillary waves at the short-wavelength side is a poor man's way to handle the otherwise diverging interface width $\langle h^2\rangle$. Figure 1 shows the function (3) together with data points referring to two experiments, denoted by II and IV [20]. The choice of δ is actually a fit of t_c. So we have plotted in the figure the data points with $t/t_c = n\delta$ and $\delta = 0.04$ for II and $\delta = 0.02$ for IV.

Although the data points follow the curve reasonably well, the scatter of the data points is manifest, and more important, though only visible in the inset, is the fact that the first few points are well below the curve. In this paper it is of less importance how well the experimental correlation function can be represented by a theoretical curve, since we are interested in the problem of directly calculating the persistence probabilities from the experimental correlation function.

4. Persistence probabilities and sum rules

To formulate the persistence probability for a discrete series, we form the $n \times n$ matrix $g_{i,j} = g_{|i-j|}$, which is determined by the first n values of g_n. Using that the process is Gaussian, the probability on a sequence of values $(h_1, \ldots, h_n)$ is given by the formula

$$G(h_1, \ldots, h_n) = \frac{1}{D^{1/2}} \exp\left(-\frac{1}{2}\sum_{i,j} J_{i,j} h_i h_j\right), \tag{4}$$

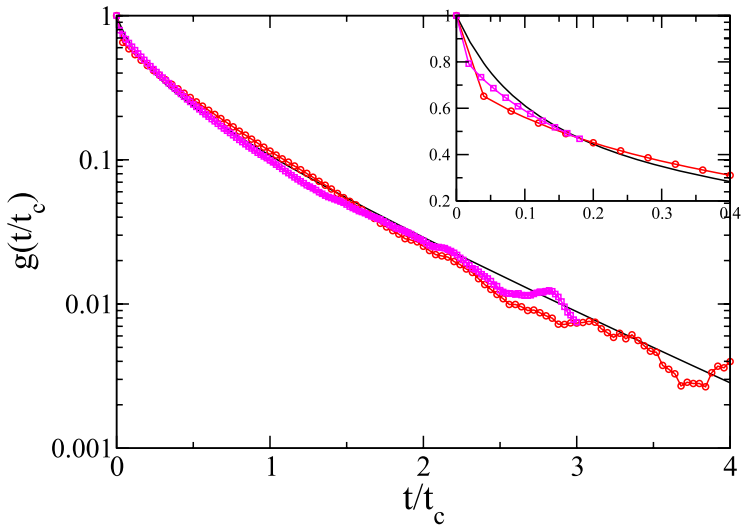

Figure 1. Height–height correlation functions, curve (3) and experimental points; circles refer to $\delta = 0.04$ (II) and squares to $\delta = 0.02$ (IV). Inset: first 10 measured correlation points and curve (3).

with the normalization $D = (2\pi)^n \det g$, where $\det g$ is the determinant of g. $J_{i,j}$ is the inverse of $g_{i,j}$, which is again an $n \times n$ matrix and its matrix elements also individually depend on n (while those of g only depend on $|i-j|$). The justification of (4) is based on the fact that the correlator $\langle h_i h_j \rangle$ as calculated with (4) does indeed lead to $g_{|i-j|}$.

The expression for the persistence probability $p_n(h)$, on a sequence of *precisely* n events above h, follows as the ratio of two integrals

$$p_n(h) = q^{-(n+)-}(h)/q^{-+}(h). \tag{5}$$

The numerator is the $(n+2)$-fold integral

$$q^{-(n+)-}(h) = \int_{\mathcal{D}} \mathrm{d}h_i \, G(h_0, \ldots, h_{n+1}), \tag{6}$$

where the integration domain $\mathcal{D}$, indicated by the superscript on q, is given by the conditions $h > h_0 > -\infty$, $h < h_i < \infty$, and $h > h_{n+1} > -\infty$. It selects the sequence of events: starting with a value below h, followed by n points above h and terminated by a value below h, which are the sequences of precisely n successive values of the height $h_i > h$. Similarly the denominator is given by the double integral

$$q^{-+}(h) = \int_{-\infty}^{h} \mathrm{d}h_0 \int_{h}^{\infty} \mathrm{d}h_1 \, G(h_0, h_1) \tag{7}$$

The inverse matrix $J_{i,j}$ depends for $n = 2$ only on the first value g_1 of the correlation function. So the $q^{-+}(h)$ is generally given by

$$q^{-+}(h) = \int_{-\infty}^{h} \mathrm{d}h_0 \int_{h}^{\infty} \mathrm{d}h_1 \, \frac{\exp[-(h_0^2 + h_1^2 - g_1 h_0 h_1)/(1-g_1^2)]}{[2\pi(1-g_1^2)]^{1/2}} \tag{8}$$

The denominator serves as the normalization, since one has the relation

$$q^{-+}(h) = \sum_{n=1} q^{-(n+)-}(h) \tag{9}$$

which gives the sum rule for the total probability

$$\sum_{n=1} p_n(h) = 1. \tag{10}$$

The derivation of (9) is based on repeated expansion of the relation

$$q^{-+}(h) = q^{-+-}(h) + q^{-++}(h) = q^{-+-}(h) + q^{-++-}(h) + q^{-+++}(h) = \cdots, \tag{11}$$

which simply states that the probability of finding a sequence $-+$ is the same as that of finding it from the events $-++$ and $-+-$. Together they extend the integration over the last height variable over all values and the probability for $-+$ results. Repeatedly adding a new point in the sequence ending with $+$ leads to the identity (9).

There exists one other sum rule. Consider $q^{+}(h)$, which is the single integral over h_0 with $h_0 > h$. The expansion, like (11), starts as

$$q^{+}(h) = q^{+-}(h) + q^{++}(h) = q^{-+-}(h) + q^{+-} + q^{-++}(h) + q^{+++}(h). \tag{12}$$

Systematically replacing every $+$ at the beginning or end of the string by the sum of strings extended with a $+$ and $-$ gives

$$q^{+}(h) = \sum_{n=1} n q^{-(n+)-}(h). \tag{13}$$

This yields for the mean value the sum rule

$$\sum_{n=1} n\, p_n(h) = q^{+}(h)/q^{-+}(h). \tag{14}$$

We have not found further sum rules.

The sum rules (10) and (14), which generally apply for stationary Gaussian processes, involve integrals which are easy to execute. $q^{+}(h)$ is an error function and $q^{-+}(h)$ can be reduced from the double integral (8) to a single integral, for which an analytic expression exists for $h = 0$ [21]

$$q^{-+}(0) = \frac{1}{2} - \frac{1}{\pi} \arctan\left(\frac{1+g_1}{1-g_1}\right)^{1/2}. \tag{15}$$

The sum rules are typical for the discrete series as the continuum limit for non-smooth processes is singular. If one could straightforwardly define in the continuum limit a probability density $p(t)$ on a persistence interval t, one would expect it to be related to the discrete p_n as

$$p(n\Delta t)\Delta t \simeq p_n, \tag{16}$$

where we suppressed the h dependence for the moment. The probability density is then normalized:

$$\int_0^\infty \mathrm{d}t\, p(t) \simeq \sum_{n=1} p_n = 1. \tag{17}$$

Consequently one would expect the mean of the discrete series to diverge as

$$\sum_{n=1} n\, p_n = (\Delta t)^{-1} \sum_{n=1} (n\Delta t)\, p_n \simeq (\Delta t)^{-1} \int_0^\infty \mathrm{d}t\, t\, p(t) \sim (\Delta t)^{-1}. \tag{18}$$

However the expression (15) shows, with $g_1 \simeq 1 - \mathcal{O}(\Delta t)$, that

$$q^{-+} \sim (\Delta t)^{1/2}, \tag{19}$$

while q^+ is independent of Δt. So the discrete mean diverges as $(\Delta t)^{-1/2}$ in contrast to the expected behavior (18). The discrepancy is due to the Brownian fluctuations on all length scales for a non-smooth correlation function [5, 20]. This gives a non-integrable probability density for short times, making the normalization (17) questionable.

We calculate the $p_n(h)$ and then check whether the total and mean correspond to the exactly calculable ratios. In particular (14) is a stringent test for the calculated values of $p_n(h)$, since it more sensitive to the large n values than (10).

The restricted integration domain prevents the integral (6) from being straightforwardly evaluated. Although it involves a finite set of integrations, which can indeed be performed by standard techniques for small n, a direct evaluation of (6) is impossible for large n. As we shall show, expression (6) has a definite asymptotic large n behavior, but the experimental data are not exclusively determined by this asymptotic behavior at all. In fact, the practical regime for which accurate data can be collected shows important transient behavior.

5. The Markovian case

Our calculational scheme is inspired by the perturbation technique of Majumdar and Sire [4], which takes the Markovian case as the lowest approximation. The Markovian case has an exponential decaying correlator

$$g(t/t_c) = \exp(-\lambda t/t_c), \tag{20}$$

such that $g_n = g^n$ with $g = \exp(-\lambda\delta)$. The inverse matrix J is then a band matrix with all elements 0 except on the diagonal:

$$J_{00} = J_{n+1,n+1} = 1/(1-g^2), \qquad J_{ii} = (1+g^2)J_{00}, \qquad J_{i,i\pm1} = -gJ_{00}. \tag{21}$$

Note that this also holds for a matrix of finite dimension n. If the matrix J is restricted to the diagonal and the subdiagonals, the corresponding joint probability can be factorized in several ways. We present here the symmetric representation for the above Markovian case

$$M(h_0, \ldots, h_{n+1}) = f_0(h_0) \left(\prod_{i=1}^{n+1} K(h_{i-1}, h_i) \right) f_0(h_{n+1}). \tag{22}$$

The initial (and final) function is given by

$$f_0(x) = \exp[-u_0 x^2]/[2\pi]^{1/2}, \tag{23}$$

with $u_0 = 1/4$. The kernel reads

$$K(x,y) = \frac{\exp[-u(x^2+y^2) + vxy]}{[2\pi(1-g^2)]^{1/2}}, \tag{24}$$

J. Stat. Mech. (2009) P09003

with the values

$$u = \frac{(1+g^2)}{4(1-g^2)}, \qquad \text{and} \qquad v = \frac{g}{(1-g^2)}. \tag{25}$$

Physically, the factorization results from the fact that in a Markovian process the probability of an event only depends on the probability of the previous event. Mathematically, any matrix which is restricted to the diagonal and the subdiagonals can be seen as a Markovian matrix. We use the more convenient symmetric form, allowed by time reversal symmetry, rather than the standard conditional probability, with an asymmetric kernel. We will lean heavily on choosing the optimal Markovian approximation, which uses optimal values for the u and v and not those tied in with g.

Any of these representations will give the values of $p_n(h)$ recursively. Define a set of functions $f_n(x)$ with $f_0(x)$ given by (23). f_1 is constructed from f_0 as

$$f_1(y) = \int_{-\infty}^{h} \mathrm{d}x\, f_0(x) K(x,y). \tag{26}$$

The general term is defined by recursion for $1 < i \leq n+1$:

$$f_i(y) = \int_{h}^{\infty} \mathrm{d}x\, f_{i-1}(x) K(x,y). \tag{27}$$

Then $p_n(h)$ can be expressed as

$$p_n(h) = \int_{-\infty}^{h} \mathrm{d}x\, f_{n+1}(x) f_0(x)/q^{-+}(h). \tag{28}$$

In the Markovian case the multiple integral (6) becomes a repeated integral transformation with K as the kernel. Asymptotically the result is dominated by the largest eigenvalue of the kernel, which then leads to a persistence exponent.

6. Calculational scheme

Our approximation scheme is based on a separation of J in a Markovian part M and a remainder H:

$$J = \mathcal{M} + \mathcal{H}. \tag{29}$$

$\mathcal{M}$ is a Markovian approximant, i.e. a matrix which is confined to the diagonal and the subdiagonals. Thus one can relate a kernel K to $\mathcal{M}$ as in (22), but with as yet unspecified values of u_0, u and v. Also a Markovian joint probability M can be associated with this part (as in (22)), which enables us to define a Markovian approximation $p_n^0(h)$:

$$p_n^0(h) = \frac{1}{q^{-+}(h)} \int_{\mathcal{D}} \mathrm{d}h_i\, M(h_0, \ldots, h_{n+1}), \tag{30}$$

with $\mathcal{D}$ the same integration domain as in (6). The full probability $p_n(h)$ then reads

$$p_n(h) = p_n^0(h) \langle \exp(-\mathcal{H}) \rangle_0. \tag{31}$$

where the average $\langle \mathcal{A} \rangle_0$ is defined as

$$\langle \mathcal{A} \rangle_0 = \frac{\int_{\mathcal{D}} \mathrm{d}h_i \, M(h_0, \ldots, h_{n+1}) A(h_0, \ldots, h_{n+1})}{\int_{\mathcal{D}} \mathrm{d}h_i \, M(h_0, \ldots, h_{n+1})}. \tag{32}$$

The exponential in (31) will be evaluated using the cumulant expansion. The Markovian average of the first cumulant of $\mathcal{H}$ and the higher cumulants are calculated in a similar iterative way to $p_n^0(h)$.

There is a large amount of freedom in choosing the Markovian part. Any matrix with only a non-zero diagonal and non-zero subdiagonals would do. This freedom can be exploited through the inequality

$$\langle \exp(-\mathcal{H}) \rangle \geq \exp(-\langle \mathcal{H} \rangle). \tag{33}$$

The optimal Markovian matrix gives the largest value for the right-hand side. The calculation thus consists of finding an optimal Markovian approximation and evaluating the corrections. For the convergence of the calculational scheme the optimization is crucial. As optimization parameters we can use u_0, and for each kernel a choice for u and v. The practical optimization is a trade-off between the optimum and calculational simplicity. It is expedient to have all kernels the same, with the exception of the first and last. They have anyway a different role, carrying the system from below h to above h, while the other propagators keep the system above h. So we are left with an initial (and final) u_0, the first (and last) pair u_1, v_1 and the bulk pair u, v. A further restriction stems from the chosen integration procedure. The integrals can be quickly and accurately evaluated using Gaussian quadrature, with a Gaussian as the weight factor. The initial $f_0(x)$ is a Gaussian. Requiring that after an iteration the asymptotic behavior is still the same Gaussian, u, v and u_0 have to be related as $u^2 = v^2 + u_0^2$. A constant Gaussian allows us to use the same positions and weights in the Gaussian quadrature for each iteration. This reduces the freedom from five to three parameters: u_0, v_1 and v.

Thus our calculational scheme starts out by finding for every n the optimal values of the parameters u_0, v_1 and v. According to the inequality (33) this gives persistence probabilities $p_n(h)$ which are too low. Consequently the total persistence and the mean as calculated with this approximation will be lower than the exact values calculated from the sum rules (10) and (14). Using the Gaussian quadrature, this is a fast routine. The next step is the calculation of the second cumulant, which leads to an overestimation of the persistence probability. Thus, including the second cumulant, the sum rules are approached from above. As the second cumulant requires one to calculate many correlation functions (going up with n^2), this has already become a longer calculation. It takes about an hour on a simple PC to calculate persistence probabilities up to $n = 150$. Needless to say, the computation of the third cumulant, where the number of correlation functions goes up as n^3, is even more time-consuming. In practice we could calculate the third cumulant up to $n = 40$ in a reasonable amount of time. Fortunately the changes in the persistence probabilities due to the inclusion of the third cumulant are so small that they do not influence the values of the sum rules.

7. Test of the approximation scheme

Before we carry out the computation of the persistence probabilities of the actual data, we inspect a clean case by taking the correlation points g_n from the analytic expression (3).

Table 1. Sum rules for the test curve; cumulants and exact values.

	II: $\delta = 0.04$			IV: $\delta = 0.02$		
Sum	First	Second	Exact	First	Second	Exact
$\sum_n p_n(0)$	0.9935	1.000 02	1.0000	0.9932	1.0005	1.0000
$\sum_n np_n(0)$	4.6998	4.851 7	4.8420	6.3623	6.5417	6.5351

This has the advantage of noise-free input and allows us to vary the sampling rate δ. The test consists of the calculation of the sum rules with the cumulant expansion outlined in the previous section. We consider two samplings of the curve (3), $\delta = 0.04$ and, twice as narrow, $\delta = 0.02$, which correspond closely to the experiments II and IV [21]). We take $\kappa = 50$ in both cases. In table 1 we have summarized the sum rules for the total (10) and mean (14) persistence in the first-cumulant and second-cumulant approximations, for the two samplings of (3) with level $h = 0$ as the discriminator. We have calculated 100 points for sampling II and 150 points for IV, which suffice for saturating the values of the sums. The third entry, exact, gives the values of the sum rules calculated from the ratios of integrals. The accuracy of the total probability according to the first cumulant, giving a rigorous lower bound, is amazing. For the mean value this is still impressive, but it indicates that the probability for the higher values of n is somewhat too low. The second cumulant, always overestimating the probabilities, makes up well for this deficiency of the lower bound. The overall impression is that the scheme performs very well for points taken from the curve (3). We have doubled the cut-off κ to see the influence. It marginally lowers the curve, except that g_1 is decreasing visibly. A larger cut-off makes the process less 'smooth'. This gives a deterioration of the bound. We have verified that including the third cumulant does not change the numbers in table 1 appreciably.

8. Comparison with the experiments

The challenge is as regards whether the calculation of the persistence probabilities from the data points of the correlation function is also accurate. First we test this again, inspecting the sum rules, which are summarized in table 2. The entry 'Exact' refers to the calculation of the sums using (10) and (14), which requires only the value of g_1. The marks around 'Exact' refer to the uncertainties in g_1 determining the ratios, which are not correlated with the uncertainty in the other g_n, together determining the persistence probabilities. The sums for state point II are based on 100 points, which is about the number of reliable values of g_n. The sums for state point IV are extended to 150 points. In both cases the value of $p_n(0)$ is then so small that inclusion of further points will not change the sums. The lower bound is considerably less accurate than for the g_n generated. This is not surprising. The above mentioned scatter in the data adds to the non-Markovian character. Even if the process were strictly Markovian, the noise would be seen as a deviation from Markovian behavior and would lead to a convergence questioning. The second reason is that the measured g_1 is quite low: $g_1 = 0.65$ (II) and $g_1 = 0.79$ (IV). We noticed that less 'smooth' processes already have a slower convergence. However the second cumulant approaches nicely the correct values, indicating that these calculated persistence probabilities are accurate.

J. Stat. Mech. (2009) P09003

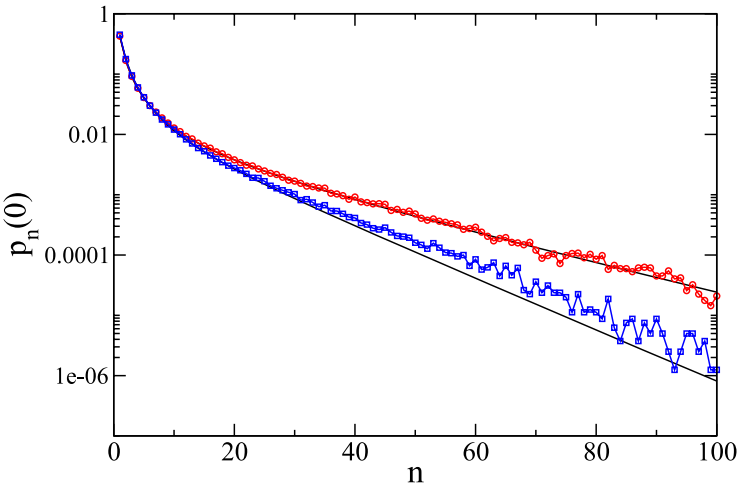

Figure 2. Probabilities (lines) calculated from the measured correlation function and measured probabilities (points) for state points II (lower curve, squares) and IV (upper curve, circles) and $h = 0$.

Table 2. Sum rules for the experiments; cumulants and calculated mean.

	State point II			State point IV		
Sum	First	Second	'Exact'	First	Second	'Exact'
$\sum_n p_n(0)$	0.9480	1.0024	1.0000	0.9339	1.0034	1.0000
$\sum_n np_n(0)$	2.8760	3.7093	3.6513	3.2761	4.9344	4.7933

The real challenge is to see how well the persistence probabilities calculated from the measured correlation points compare with measured probabilities. This is shown figure 2 for the two state points (with $h = 0$). The calculated points are taken from the second-cumulant approximation, since the third cumulant has no appreciable influence. The agreement for state point IV is as good as one can hope for with probabilities as small as 10^{-5}. For state point II there is a systematic deviation for larger n. This may be caused by artifacts resulting from the confocal slicing. $\langle h^2 \rangle$ and, therefore, the resolution relative to $\langle h^2 \rangle$ are higher for IV than for II, leading to more pronounced artifacts in II [20]. Note that the asymptotic exponential decay sets in around $n = 30$, which takes as long as 15 s in real time.

9. Discussion

We have presented measurements for the correlation function and the persistence probability of the fluctuating heights of a colloidal interface. We have developed a calculational scheme which enables us to find the persistence probability directly from the measured correlation function. This means that our scheme is independent of the agreement of the correlation function with a function like (3). The only assumption is that the distribution (4) is Gaussian, which stems from the fact that the thermal interface fluctuations are small deviations from equilibrium. The predictions of the persistence

J. Stat. Mech. (2009) P09003

probabilities from the measured correlation function agree very well with the measured persistence probabilities.

Finally we would like to make a few comments on the results.

(1) Figure 2 shows that the curve approaches an exponential decay, albeit a window from 30–100 points not being large enough for an accurate determination of the exponent. As we mentioned, the two experiments may be seen as two samplings of the same correlation function. In order to compare the two samplings we translate the behavior to the time domain. For the two samplings we estimate the decay of $p_n(0) \sim \exp(-\psi(\delta)n)$. Since $n\delta = t/t_c$, the persistence exponent θ equals $\theta = \psi(\delta)/\delta$. For the smallest δ we find $\theta = 0.027$ and for the larger δ, $\theta = 0.026$. These two values need not be the same. As observed by Ehrhardt *et al* [17], the exponent for non-smooth processes is quite sensitive to the sampling rate. The discrete series does not record what happens *in between* the measured points. The continuous process might dive below the level h between recorded points. Such paths are excluded in a continuous formulation, but are included in the discrete version [16, 20]. This leads to a smaller exponent for a larger δ.

(2) We note that we cannot take the continuum limit for practical and essential reasons. Making our δ smaller requires longer series to be calculated as the two samplings show. But more importantly, a smaller δ will lead to a more sharply peaked kernel, which ultimately has to approach a δ-function. Such a delta peak cannot be treated by Gaussian quadrature, which has helped to speed up the integrations by about a factor of a thousand with respect to e.g. a Simpson rule.

(3) We have checked that higher cumulants have virtually no influence on the persistence probabilities calculated here. We noticed, however, that although the third cumulant is small, it develops a linear dependence on n. It has no influence on the sum rule results presented or on the persistence probabilities presented, since it changes only the probabilities which are already too small to contribute. But it will have a non-negligible influence on the decay exponent of the discrete series, showing up in a region which is beyond our measurements. This also means that the experiments have not entered the fully developed asymptotic regime.

Acknowledgments

The authors wish to thank Wim van Saarloos and Henk Hilhorst for stimulating discussions.

References

[1] Slepian D, 1962 *Bell Syst. Technol.* **41** 463
[2] Kac M, 1962 *SIAM (Soc. Ind. Appl. Math.) Rev.* **4** 1
[3] Blake I F and Lindsey W C, 1973 *IEEE Trans. Inf. Theory* **19** 295
[4] Majumdar S N and Sire C, 1996 *Phys. Rev. Lett.* **77** 1420
[5] Krug J, Kallabis H, Majumdar S N, Cornell S J, Bray A J and Sire C, 1997 *Phys. Rev.* E **56** 2702
[6] Majumdar S N, Sire C, Bray A J and Cornell S J, 1996 *Phys. Rev. Lett.* **77** 2867
[7] Newman T J and Torockzai Z, 1998 *Phys. Rev.* E **58** R2685
[8] Hilhorst H J, 2000 *Physica* A **277** 124
[9] Derrida B, Bray A J and Godreche C, 1994 *J. Phys. A: Math. Gen.* **27** L37
[10] Derrida B, Hakim V and Pasquier V, 1995 *Phys. Rev. Lett.* **75** 751

J. Stat. Mech. (2009) P09003

[11] Derrida B, Hakim V and Zeitak R, 1996 *Phys. Rev. Lett.* **77** 2871
[12] Majumdar S N and Bray A J, 1998 *Phys. Rev. Lett.* **81** 2626
[13] Dougherty D B, Lyubinetsky I, Wiliams E D, Constantin M, Dasgupta C and Das Sarma S, 2002 *Phys. Rev. Lett.* **89** 136102
[14] Kallabis H and Krug J, 1999 *Europhys. Lett.* **45** 20
[15] Constantin M, Dasgupta C, Das Sarma S, Dougherty D B and Williams E D, 2007 *J. Stat. Mech.* P07011
[16] Majumdar S N, Bray A J and Ehrhardt G C M A, 2001 *Phys. Rev.* E **64** 015101
[17] Ehrhardt G C M A, Bray A J and Majumdar S N, 2002 *Phys. Rev.* E **65** 041102
[18] Oerding K, Cornell S J and Bray A J, 1997 *Phys. Rev.* E **56** R25
[19] Deloubrière O and Hilhorst H J, 2000 *J. Phys. A: Math. Gen.* **33** 1993
[20] de Villeneuve V W A, van Leeuwen J M J, de Folter J W J, Aarts D G A L, van Saarloos W and Lekkerkerker H N W, 2008 *Europhys. Lett.* **81** 60004
[21] de Villeneuve V W A, van Leeuwen J M J, van Saarloos W and Lekkerkerker H N W, 2008 *J. Chem. Phys.* **129** 164710
[22] Aarts D G A L, Schmidt M and Lekkerkerker H N W, 2004 *Science* **304** 847
[23] Royal C P, Aarts D G A L and Tanaka H, 2007 *Nat. Phys.* **3** 636
[24] Lekkerkerker H N W, Poon W C K, Pusey P N, Stroobants A and Warren P B, *Phase behavior of colloid + polymer mixtures*, 1992 *Europhys. Lett.* **20** 559
[25] Jeng U, Esibov S, Crow L and Steyerl A, 1998 *J. Phys.: Condens. Matter* **10** 4955

J. Stat. Mech. (2009) P09003